The effect of Pt surface orientation on the oscillatory electro-oxidation of glycerol

Vinicius Del Colle[a,b*], Gabriel Melle[b,c], Bruno A.F. Previdello[d], Juan M. Feliu[c], Hamilton Varela[b], Germano Tremiliosi-Filho[b]

[a] Department of Chemistry, Federal University of Alagoas-Campus Arapiraca, Av. Manoel Severino Barbosa s/n, 57309-005 – Arapiraca, Alagoas, Brazil.

[b] São Carlos Institute of Chemistry, University of São Paulo, Av. Trabalhador São Carlense, 400, 13566-590 – São Carlos, São Paulo, Brazil.

[c] Instituto de Electroquímica, Universidad de Alicante, Apdo. 99, E- 03080, Alicante, Spain.

[d] Instituto Senai de Inovação em Biomassa, Rua Angelina Tebet, 777, 79640-250 – Três Lagoas, MS, Brazil.

Authors Orcid:

V. Del Colle (http://orcid.org/0000-0001-8595-5129)

G. B. Melle (https://orcid.org/0000-0001-7925-2224)

B. A. F. Previdello (https://orcid.org/0000-0001-5292-7957)

J. M. Feliu (https://orcid.org/0000-0003-4751-3279)

H. Varela (https://orcid.org/0000-0002-6237-6068)

G. Tremiliosi-Filho (http://orcid.org/0000-0001-9162-3438)

*Corresponding author.

E-mail address: delcolle@arapiraca.ufal.br (V. Del Colle).

Abstract

In the present paper, we have studied the influence of (bi)sulfate anion (0.1 and 0.5 M) on the electro-oxidation of glycerol on basal Pt(*hkl*) and stepped surfaces belonging to the series of Pt(S)[*n*(111) x (111)]. Cyclic voltammograms and derivative voltammetry pointed out that the catalytic activity decreases for Pt(111) and Pt(110) and, to a minor extent, for stepped surfaces in 0.5 M H_2SO_4. Chronoamperometric curves demonstrated that above 0.60 V (*vs.* RHE), for both concentrations (0.1 and 0.5 M H_2SO_4), stepped surfaces and Pt(110) showed greater ability to catalyze the glycerol electro-oxidation in comparison with Pt(111). Potential oscillations were mapped along with slow galvanodynamic sweeps and studied at constant current. For Pt(111), no oscillations were found in the galvanodynamic regime, however, under the galvanostatic regime, period 1 oscillations were observed after a long induction period. The oscillations showed a very similar profile for stepped surfaces, even for a surface with a high step density (110), such as Pt(332). Pattern changes were observed only for Pt(110) compared to other surfaces. Therefore, we conclude that (110) step sites influence the oscillatory behavior, thus the insertion of the steps favors the path of formation of inactive species, which compete for the same catalytic sites in a given potential region. The extinction of the mechanism oscillatory occurs differently due to the intrinsic characteristics of each surface electrode for the formation of (hydro)oxides.

***Keywords**:* Glycerol electro-oxidation; Electrolyte concentration; basal Pt(*hkl*); Stepped Surfaces; Cyclic Voltammetry; Chronoamperometry; Potential oscillations.

1. Introduction

The great appeal in studying electro-oxidation of small organic molecules consists mainly of the high theoretical energy densities, low toxicity, considerable reactivity, and easy handling because these fuels are liquids at room temperature [1]. Among the main organic molecules in the context of electrocatalysis, glycerol has attracted attention due to its promising use in fuel cells, since its complete oxidation releases $14e^-$ per molecule [2,3]. This alcohol is produced at low cost and on a large scale as a coproduct from biodiesel. In this sense, most works dedicate their efforts to design an electrocatalyst that could improve the route that enhances CO_2 production and seek a way to circumvent the poisoning intermediates formed during the reaction [4,5]. Another promising application considers its use as a starting reagent for the electrochemical production of valuable chemicals, such as dihydroxyacetone, glyceric acid, and tartronic acid [6], as well as its use in an electrochemical reactor, to generate hydrogen as the main source of energy [7,8].

Alcohol electro-oxidation reactions are fully dependent and sensitive to the surface structure of the electrocatalyst, supporting electrolyte, electrolyte concentration, temperature, applied potential, and different species that might be formed on the electrode interface [3]. Del Colle et al. reported that the glycerol electro-oxidation reaction (GEOR) is influenced by crystallographic structure [9], namely, stepped surfaces influence decisively the surface reactivity, and the species formed are determined by the difference between the width of (111) terraces and (110) monoatomic steps. According to the authors, Pt(111) has shown the higher electroactivity towards GEOR, while Pt(110) has demonstrated a more remarkable ability to break C-C bonds to convert into CO_2. Incidentally, a stepped surface having 10 atoms-wide terraces is more selective to form only C3 products such as dihydroxyacetone, glycolic acid, and glyceric acid [9].

The main difficulty in direct alcohol fuel cells (DAFC) is the low practical current density obtained due to the self-poisoning by strongly adsorbed reaction intermediate species on the electrode surface [10]. These species can be CO_{ads} and $R - CH_{x,ads}$ carbonated species with R containing one or two carbon atoms, depending on the alcohol. Another limitation is the necessity of high potentials to break the C–C bond. These problems represent barriers to the total oxidation of alcohols to CO_2 [2,3]. Studying electrocatalytic systems under oscillatory regime might be of help in discriminating mechanistic details [11], but only a few works have reported GEOR behavior concerning oscillation instabilities. Therefore, the most organic oxidation reaction is feasible to find potential oscillations [12–15]. Oliveira et al. [12] report for the first-time oscillatory behavior present on GEOR on polycrystalline platinum in acid medium with different concentrations. The authors observed potential instabilities in the region between 0.40 and 0.80 V (*vs.* RHE). Although the oscillations show a rather conventional behavior, with a majority of period 1 (P1), the oscillatory series duration was affected by the glycerol concentration, and a decrease from 0.2 to 0.1 M of glycerol resulted in a duration 50% shorter.

Kwon et al. [16] elucidated the mechanism of GEOR on platinum by combining high-performance liquid chromatography (HPLC) with linear voltammetry. The authors identified that glyceraldehyde, together with glycolic acid and dihydroxyacetone, the latter in smaller quantities, are the main products generated at $E < 1.0$ V (*vs.* RHE). Thus, the authors propose that the glycerol oxidation path goes through glyceraldehyde and glycolic acid formation, respectively, as the first products of partial glycerol oxidation.

Subsequently, the impact of these partially oxidized soluble intermediates on the GEOR was studied by Melle et al. [13] under voltammetric and oscillatory regimes. In this work, using a rotating disk electrode, the authors showed that the voltammetric region was inhibited at $E <$ 0.60 V (*vs.* RHE), resulting in the surface electrode poisoning through the oxidation of partially

oxidized soluble species. The electrode rotation removes these soluble species from the vicinity, making it difficult to return to the surfaces and their further oxidation to strongly adsorbed species. Consequently, a new faradaic process was observed in the voltammogram at a potential lower than 0.55 V due to glycerol oxidation on a non-poisoned surface. Under the oscillatory regime, they observed that the concentration decrease of these soluble intermediates in the electrode vicinity directly impacted the oscillation duration.

In the present work, we report the GEOR on basal Pt(*hkl*) and stepped surfaces of type Pt(S)[*n*(111) x (110)] at different (bi)sulfate concentrations. The study was carried out using cyclic voltammetry and chronoamperometry. Potential oscillations were mapped and investigated under galvanodynamic and galvanostatic regimes, respectively. The results were discussed in connection with voltammetric and chronoamperometric data.

2. Experimental

All Pt electrodes, low and high Miller index, used in this work were cut and polished from small single crystal platinum beads following the procedure described by Clavilier [17]. The stepped surfaces, Pt(776), Pt(554), and Pt(332), belong to the series of Pt(S)[*n*(111) x (111)] or can also be represented as Pt (S)[(*n*−1)(111) × (110)] because the junction of a (111) step site with the (111) terrace forms a step with site (110) symmetry. These surfaces have 14, 10, and 6 atom-wide terraces. Since the intersection of a (111) terrace and a (111) step also defines a (110) site, these electrodes can also be described as a combination of (*n* - 1) atom-wide (111) terraces and (110) monoatomic steps. The electrodes were cleaned by flame annealing, cooled down in an H_2/Ar atmosphere, and protected with water in equilibrium with this gas mixture to prevent contamination before immersion in the electrochemical cell, as described elsewhere [18]. It is known that this procedure leads to well-ordered surfaces having nominal terrace lengths separated by monoatomic steps [19].

All experiments were performed at 25ºC in a conventional three-electrode electrochemical cell. The chemicals used for solution preparations were of high purity: sulfuric acid (Panreac, 99.98%), Glycerol (Sygma-Aldrich, 99.99%), and ultrapure water (18.2 MΩ cm, Millipore). The counter electrode was a 1 cm × 1 cm platinized Pt foil. The reference electrode was a reversible hydrogen electrode (RHE) in the same electrolyte solution, separated from the main cell, and all potentials in this work are referred to it. The electrochemical measurements were performed with a Metrohm-Autolab Potentiostat/Galvanostat PGSTAT-302N. The electrode was immersed in 0.2 M glycerol + 0.1 or 0.5 M H_2SO_4 solutions deareted with Argon (99.999%) for the GEOR studies. During this process, the electrode was polarized at 0.1 V for 10 s. After this, the voltammetric study was performed in the potential range of 0.05-0.9 V at 0.02 V s^{-1}. Before galvanostatic/dynamic experiments, the electrodes were submitted to one voltammetric cycle in the electrolyte solutions. All Pt electrodes used in the present study were checked in acid media (see Fig. SI1 in the supporting information), the electrochemical characterization recorded indicated a high degree of surface crystalline order and cleanliness of the system, as seen detailed in elsewhere [20].

3. Results and Discussion

3.1 Cyclic voltammetry

After each typical surface characterization step in electrolyte media [20], the first scan of glycerol electro-oxidation was recorded (Fig. 1A-B) for the two electrolyte concentrations selected (0.1/0.5 M H_2SO_4). The anodic profile of glycerol oxidation on Pt(111) in 0.1 M H_2SO_4 showed no current below 0.32 V due to strong hydrogen adsorption at low potentials, as seen by the small hydrogen adsorption peak. After that, the current density increases and exhibits a first, intense peak, at 0.57 V. For Pt(111) in 0.5 M H_2SO_4, the onset potential is displaced to a more positive potential, and the shoulder at 0.70 V, is relatively more pronounced than in 0.1

M H_2SO_4. The main peak observed at 0.57 V decreases significantly, by 4 times, indicating that the anion adsorption affects the reaction mechanism.

For stepped surfaces, the current density values decrease with the addition of steps, the highest activity being observed for Pt(111), and the lowest one for Pt(110). According to Del Colle et al. [9], GEOR mechanism for Pt(S)[*n*(111) x (111)] electrodes can be represented as a linear combination of the terrace and step sites as independent variables. The presence of two oxidation peaks in the positive scan direction can be assigned to (111) oriented terraces at 0.58 V and the second peak, at 0.70 V, to the (110) monoatomic step.

The CVs evidence the influence of sulfate adsorption on the GEOR, the changes provoked by increasing electrolyte concentration affect the performance of the reaction rate. The electroactivity for Pt(111) in 0.5 M of H_2SO_4 is altered when compared to 0.1 M H_2SO_4, where the current density decreases significantly. For the stepped surfaces, the onset potential is shifted to more positive potentials when high electrolyte concentration is used, except for Pt(332), having 6 atom-wide terraces, in which the CV anodic profiles are very similar for both concentrations.

In this case, the reaction inhibition becomes less significant as step density increases. This fact is supported by competition between sulfate adsorption and the formation of $(OH)_{ads}$ species on these surfaces when the potential increases. Herrero et al. [21] showed that the Gibbs excess of anion adsorption for a family of stepped Pt(*hkl*) surfaces in solutions of H_2SO_4 decreased with the increases in step density, i.e. the anion adsorption is stronger at larger (111) terraces. Another interesting point is that the adsorption of sulfate on Pt(111) starts after the end of the hydrogen region, increasing with the increase of the potential, up to a maximum value of approximately 3×10^{14} ions cm^{-2}. It is worth mentioning that the phase transition associated with the sharp peak at 0.49 V (Fig. SI1) occurs exactly where the coverage of sulfate reaches its maximum value [22].

It is known that the surface structure of the sites determines the adsorption geometry. The most likely symmetry for sulfate in Pt(111) is C_{3v}, due to the correlation between oxygen-oxygen distances and Pt atoms in the hexagonal packaging of the face (111) [23,24]. While for Pt(110) and Pt(100) the adsorption via two oxygen atoms is preferential due to the symmetry of these surfaces [25,26]. An analysis of the GEOR on Pt(110) showed that the onset is shifted for more positive potentials, and the main peak *ca.* 0.80 V decreases significantly in 0.5 M H_2SO_4.

The reverse scan, for all surfaces, is presented in Fig. 1B. The hysteresis effect is a common phenomenon observed during the oxidation of small organic molecules [27–29]. The hysteresis brings information about the intermediates products formed during the reaction, mainly those that adsorb strongly at the surface, as CO_{ad} species, either observed for other organic molecules electro-oxidation on platinum surfaces [27,28]. Just as was observed for the positive-going scan, the profiles are significatively affected by anion concentration over the applied potential. Also, for 0.5 M H_2SO_4, the current densities obtained were lower. In this case, anion adsorption competes with glycerol reaction in a greater extension at the positive potentials. The only exception is observed for Pt(332), which seems to exert a strong influence in disrupting the strength of anion on the surface and originating a very close electroactivity for both concentrations [21,23–26,30].

The influence of the surface structure, namely basal planes, and stepped surfaces, on the electro-oxidation of small organic molecules, has revealed an interesting aspect of these surfaces' electroactivities. For instance, the electro-oxidation of methanol and ethanol is favored over (110) steps on the (111) terraces [20,31,32], because the steps catalyze the reaction at low potentials as well as promote the oxidation of the CO species formed. However, the same effect is not observed for GEOR, wherein the reaction is considerably affected at a low potential, and the currents decay linearly with the addition of (110) step sites [9].

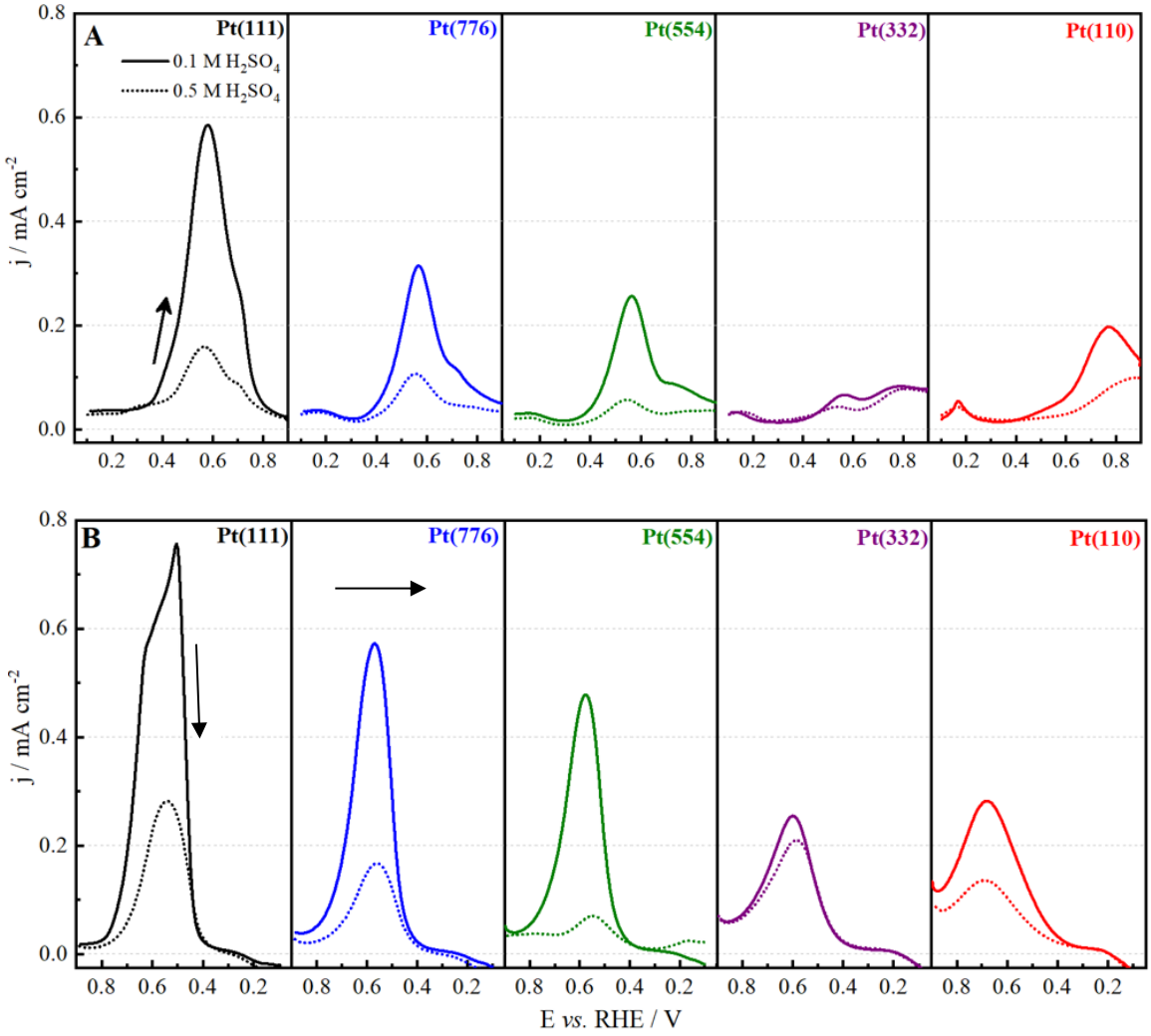

Fig. 1. 1st scan of glycerol (0.2 M) electro-oxidation reaction in acid media: (A) positive-going scan and (B) negative-going scan for: Pt(111), Pt(776), Pt(554), Pt(332) and Pt(110). Scan rate: 0.05 V s^{-1}.

An analysis of the reverse scan of Pt(111) (Fig. 1B,), for 0.5 M H_2SO_4, showed a symmetric profile, while for 0.1 M H_2SO_4 the ascendant currents exhibit a shoulder at 0.63 V with a current density above 0.55 mA cm^{-2}, generating an asymmetric shape, and after reaching a peak current at 0.50 V, it drops quickly. Pt(111) presented the highest value of current density among all surfaces studied for both concentrations. Analysis for all surfaces showed that Pt(111) obtained the highest value (0.76 mA cm^{-2}) in 0.1 M H_2SO_4, while Pt(332) presented the

lowest one (0.26 mA cm^{-2}), indicating that this surface is deactivated strongly at low potential, likely by CO_{ad} formation [9].

According to FTIR results [9], the (111) terraces are responsible for forming species containing C=O (aldehyde, ketone, or carboxyl group), namely C_3 glycerol byproducts, while the (110) step sites contribute to cleavage of the C–C bond. In this scenario, the currents in the CV represent different processes occurring and competing simultaneously on the electrode surface. In this case, the (111) terraces favor C_3 species intermediates formation, which diminishes with the addition of (110) step sites and, concomitantly onto this latter, occurs a more significant formation of species containing C_1, mainly, (CO_{linear}), while for the Pt(332) surface, a very small contribution of C_3 species is observed. Finally, when Pt(110) surface is considered, the first peak at 0.56 V disappears, and in this sense, the glycerol molecule is broken more easily at low potential and, this surface is being covered by species mostly containing C_1 [9].

For all studied surfaces, the backward currents showed higher values compared to the forward scan, this effect is called hysteresis [9], commonly observed for alcohol oxidation over Pt electrodes. The hysteresis is associated with the formation of strongly adsorbed species, mainly CO, that are formed on the electrode surface at low potentials. These species remain on the electrode surface and only at potentials above 0.6 – 0.7 V are oxidized. At the upper potential limit of the scan, the surface is free from those species and, for this reason, the currents on the negative-going scan are higher than those measured in the positive-going scan. The hysteresis brings important information about the intermediates formed during the positive scan and is quite dependent on the surface structure, once each surface forms different intermediates and consequently different pathways [9,33,34].

Therefore, a comparison among surfaces studied in different electrolyte concentrations suggests that sulfate adsorption might alter the mechanism of glycerol reaction due to changes

in the electroactivity and the onset potential. As indicated by the literature, $(OH)_{ads}$ and sulfate adsorption must be considered actors by influencing the GEOR mechanism significantly, and its performance depends on the potential and geometry of the surface. We have used a derivative strategy to better point out the faradaic process through the onset potential of GEOR. The application of dj/dE allows us to gain some details, that, normally are not observed directly from CVs, and gives us more clarity concerning the data's interpretation [35]. Thus, Fig. 2 presents the derivative current density obtained from CVs presented in Fig. 1.

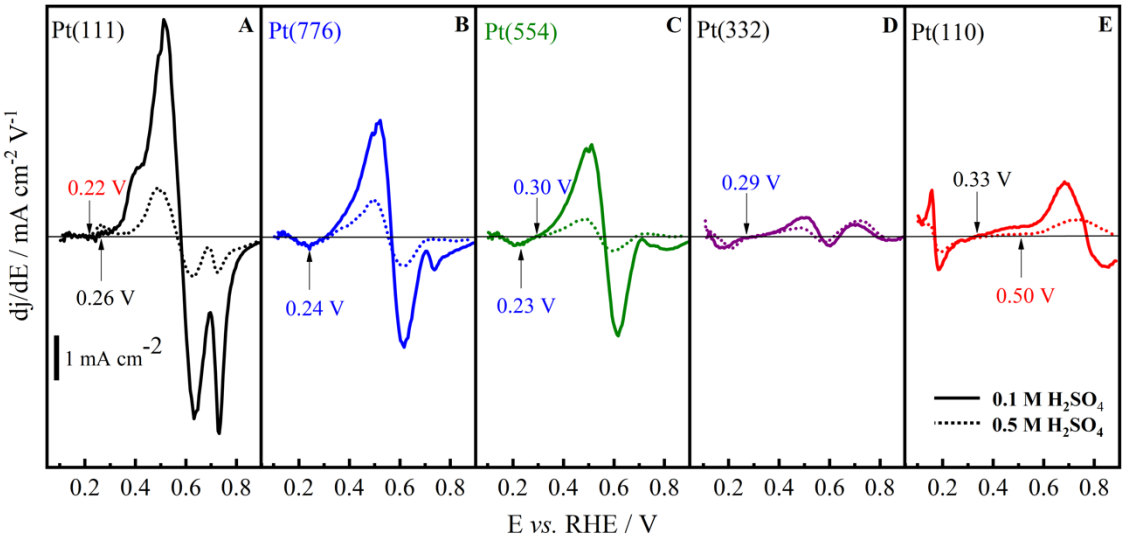

Fig. 2. A-E. Derivative of the current density as a function of the applied potential obtained from 1st scan of glycerol (0.2 M) electro-oxidation reaction in acid media for Pt(111), Pt(776), Pt(554), Pt(332), and Pt(110). Sweep rate 0.05 V s^{-1}.

According to Fig. 2A, an analysis for Pt(111) in high electrolyte concentration presented a small peak at 0.26 V and, a second one can be seen at 0.48 V. For low electrolyte concentration, a shoulder rises at 0.41 V, and an intense peak is seen at 0.51 V. A comparison between them showed a strong impact of electrolyte concentration over GEOR. The peak at 0.51 V decreases significantly as the sulfate adsorption is increased on the surface; a competition between anion and glycerol adsorption is evident and affects the reaction.

As pointed out by Del Colle et al. [9], different ketone and aldehydes species might be generated quickly at a low potential, namely, glyceraldehyde and dihydroxyacetone are the

species that are generated at the first step of the reaction. Anion adsorption delays the C3 glycerol byproducts formation to more positive potentials and in smaller amounts, since the current densities decay by about 4.5 times. Therefore, sulfate adsorption strength increases and competes with the $(OH)_{ads}$ from water and GEOR products for Pt surface sites.

A comparison of the derivative CVs for glycerol oxidation on stepped surfaces (Fig. 2B-D) showed that the inhibition of the reaction caused by anions becomes less intense as the step density increases because the current densities at high concentration of electrolyte did not decay as considerably as compared with those obtained in 0.1 M H_2SO_4. The onset potential for these surfaces practically starts at the same potential at *ca*. 0.23 V, and the mean peak intensity at 0.50 V decays when the anion concentration increases.

Fig. 3 presents the derivative current density peak values obtained from the main peak at 0.50 V, as shown in Fig. 2A-E. The amount of anion on the surface affects the faradaic current for this process and consequently, the intermediates formed at this potential may be affected. However, the increase of step densities diminishes the impact of anion adsorption and for these surfaces, the onset potential is not as affected as on Pt(111) surface. However, the electroactivity decays reaching a lower value for Pt(332), for this surface the higher concentration of anion practically is irrelevant, because the current obtained are identical. Therefore, concerning the influence of anion concentration, the GEOR is affected drastically, once the peak current is affected drastically.

The step sites can break the anion adsorption strength and mitigate the drop of the current densities for 0.5 M H_2SO_4 (dotted line). This fact corroborates the results of Mostany et al. [36], in which the Gibbs excess of anion adsorption for stepped surfaces in the sulfuric acid solution decreased with the increase of step sites.

For Pt(110), the onset potential starts at 0.33 V for low acid concentration, while in 0.5 M H_2SO_4 the current densities are shifted to 0.50V. In this case, the electrolyte concentration

significantly influences the glycerol reaction, preventing the adsorption of reactive species on the surface. Even the mean peak at 0.68 V observed for 0.1 M H_2SO_4 loses its definition and intensity when the anion concentration is increased (Fig. 2E).

According to spectroscopic studies [9], this surface demonstrated a greater capacity to break the C–C bond and the subsequent conversion into CO_2. It seems that the increase of adsorbed sulfate inhibits the glycerol adsorption and that in turn shifts the onset potential to more positive values. The analysis using derivative current density allowed us to visualize the beginning of the onset potential and the peak potential observed in the CVs (Fig. 1).

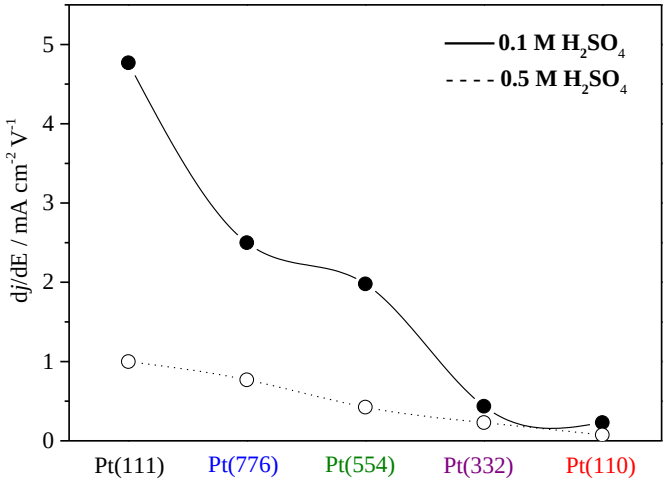

Fig. 3. The maximum value of the derivative obtained from the first peak at *ca.* 0.50 V presented in the Fig. 2A-E for: Pt(111), Pt(776), Pt(554), Pt(332) and Pt(110).

3.2 Chronoamperometry

The chronoamperometric experiments were carried out to analyze the electrochemical behavior of GEOR after potential polarization for 600 s in 0.1 and 0.5 M H_2SO_4 solution. The long-time transients were enough to achieve a *quasi*-steady-state current and evaluate the surface deactivation, as can be seen in Fig. SI2. Fig. 4 shows the current densities collected at 600 s, from each chronoamperometric curve after applying four different potentials: 0.60; 0.70; 0.80, and 0.90 V.

Fig. 4A reveals the behavior of surfaces in 0.1 M H_2SO_4. Pt(111) at 0.60 V has the highest current density among all surfaces, this great electroactivity corroborates with the CV (Fig. 1A, black curve), which in this region is obtained the higher activity. However, the performance of this surface decays abruptly when the potential is jumped to higher values, indicating surface deactivation by intermediates strongly adsorbed.

The analysis in 0.5 M H_2SO_4 (Fig. 1B) showed that for long-term electro-oxidation experiments, the Pt(111) electrode has a current density value, after polarization for 600 s, close to the stepped surfaces, in agreement with CVs obtained in Fig. 1A. This interesting point leads to the conclusion that sulfate concentration difficult the glycerol adsorption and its subsequent oxidation reaction towards dehydrogenated species with a carbonyl group. As was reported in the literature [9], Pt(111) has shown the higher electroactivity towards glycerol electro-oxidation and, during the CV positive going-scan, the onset potential for the reaction is closely related to the increase of carbonyl-containing species (C=O from aldehydes or ketones intermediates) along with CO_2 production and the same time with CO_{ad} diminution.

Another relevant fact was seen for Pt(110) (Fig. 4A). This surface reaches considerable performance after polarization at different potentials, showing better values of current densities among all surfaces studied. This result suggests that Pt(110) demonstrated greater ability in breaking the C–C bond, and the surface seems not to suffer significant deactivation as presented for other surfaces [9].

The behavior for stepped surfaces is very similar, and the electroactivity is lower and affected by monoatomic steps. A reasonable explanation to justify these surfaces' performance lies in the fact that above 0.60 V the carbonyl species formation is intensified at the end of the first cycle [9]. However, considering Pt(332) as the surface closest to Pt(110), once the surface has 6 atoms-wide terraces, it presented the highest performance among the stepped surfaces studied. Therefore, either (110) step sites and (111) terraces atoms play an important role in the

selectivity of glycerol electro-oxidation reaction. There is a tuning in the composition of the species formed along with the potential as the terraces become narrower or the number of monoatomic steps increases. Then, a flat surface like (111) favors C3 intermediates, while a stepped surface acts to favor species that came from C–C breaking until reaching (110) surface that demonstrates the greatest C–C bond-breaking ability [9].

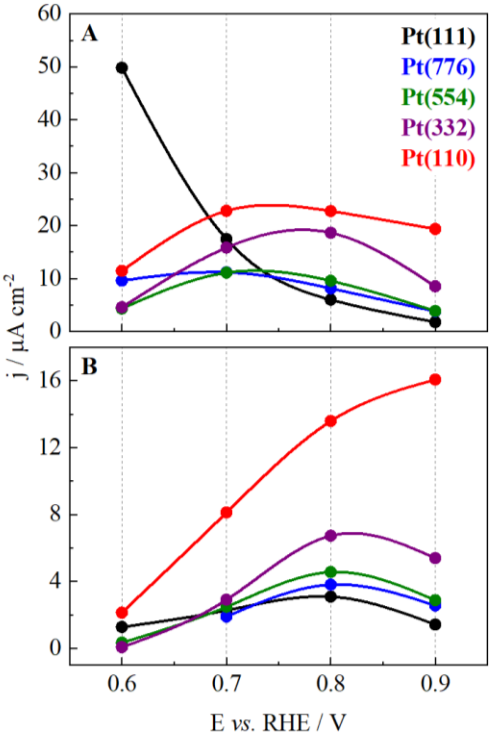

Fig. 4. Current density values collected after 600 s of polarization at different potentials for glycerol electro-oxidation obtained from chronoamperometric experiments in different electrolyte concentrations (A) 0.1 M H_2SO_4 + 0.2 M Gly and (B) 0.5 M H_2SO_4 + 0.2 M Gly, for different surfaces: Pt(111), Pt(776), Pt(554), Pt(332) and Pt(110).

The current density analysis in Fig. 4B, in 0.5 M H_2SO_4, shows a significant change in the profile compared to values obtained in a lower concentration, Fig. 4A. Pt(111) electrode at 0.60 V have not the best activity as was observed previously in Fig. 4A, and, even, the activity for the higher potentials is smaller than other surfaces studied. Considering Pt(110), this, in turn, has the best performance for glycerol electro-oxidation reaction in all polarization potentials, and no deactivation is observed over the applied potentials, reaching a maximum

value at 0.90 V. The Pt(332) surface follow the same trend, but the values are smaller than Pt(110) and a maximum activity is reached at 0.80 V. This behavior is similar for other stepped surfaces, but the current densities obtained are higher than those of Pt(111). Some remarks about the influence of electrolyte concentration reveal highlights about how the glycerol mechanism is deeply affected. The anion adsorption governs the surface performance, and long-time transient experiments allow us to evaluate surface deactivation. In the present study, the presence of sulfate in a larger concentration changes the intermediate formation producing more active species on the Pt(110). Considering FTIR studies [9], it seems evident that more species containing C2 and C1 intermediates are more easily formed on this surface.

3.3 Potential Oscillations

Dynamic instabilities in electrocatalytic systems usually result from the competition between active and non-active (poisoning) species in the same range of potential, and small changes in the electrode atomic surface structure can modify the surface adsorbates, leading to morphological change or even the extinction of oscillations. Despite the electrolyte concentration showing changes in voltammetric currents, under the oscillatory regime, no substantial changes were observed as can be seen in Fig. SI3 (0.1 M H_2SO_4 + 0.2 M Gly). For this reason, we decided to show the results for 0.5 M H_2SO_4 to investigate the surface crystallographic orientation effect associated with the GEOR in an oscillatory regime.

To study potential oscillations, the system was submitted to a slow current sweep, at 6.0 μA s^{-1}, to find the potential oscillation region. These results, known as galvanodynamic curves, are shown in Fig. 5. Potential instabilities were not detected under galvanodynamic regime for GEOR on Pt(111) surface. In contrast, Pt(776), Pt(554), and Pt(332) presented potential instability between 0.4 and 0.8 V, which coincides with the same potential range of the voltammetric peaks (see Fig. 1).

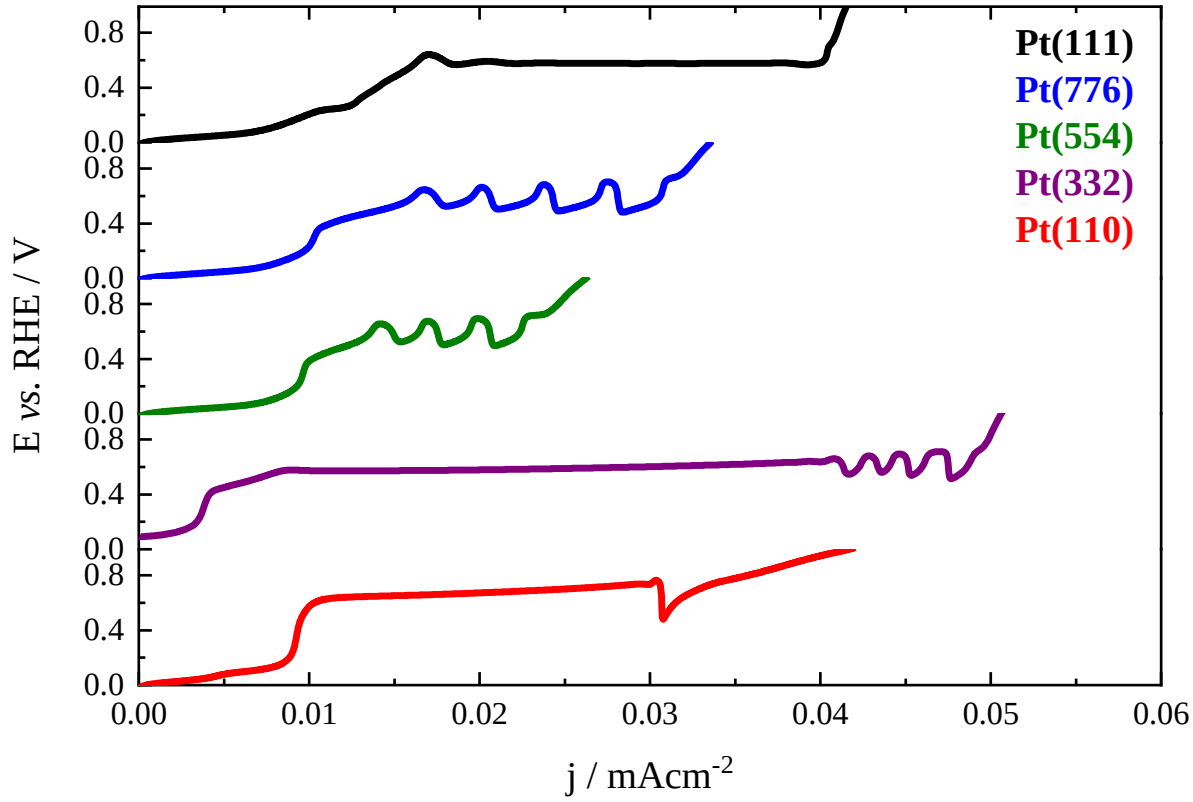

Fig. 5. Galvanodynamic curves at 6.0 μA s^{-1} for distinct surfaces during GEOR (0.5 M H_2SO_4 + Gly 0.2 M).

Pt(111) and Pt(110) showed practically no regular oscillations for GEOR, increasing (110) step sites on (111) terrace, oscillation cycles become more stable for (554), (776), and (332) surfaces. The galvanodynamic profiles on surfaces (776), (554), and (332) were quite similar to the results observed for GEOR in Pt polycrystalline [12,14]. The potential increased quickly at the beginning and the end of the oscillation series, named here pre and post-oscillation regions.

A similar strategy presented in references [37–40] was used in the present study to study the system under galvanostatic regime. Galvanostatic time-series (GTS), with a constant current in the oscillation region, were carried out to observe the potential evolution through the fixed current values on the system for Pt(111), Pt(776), Pt(554), Pt(332) and Pt(110). All studied surfaces presented oscillatory patterns for GEOR under the galvanostatic regime. Even though

some surfaces did not show oscillations in galvanodynamic regime, we decided to apply different currents to observe possible oscillations under a constant current regime.

Fig. 6 presents the GTS for GEOR on Pt(111) surface under (A1) 0.011 (A2) 0.022 and (A3) 0.044 mA cm^{-2}. Unlike the absence of oscillatory behavior observed for the galvanodynamic regime, herein, oscillations emerge at 0.57 V, after induction time, at 0.011 and 0.022 mA cm^{-2}. Only period-1 (P1) type oscillations were observed at a range of 0.48 and 0.71 V and, the oscillations are finished with a rapid increase of potential up to 0.9 V.

As previously reported [41], the GEOR on Pt(111) occurs initially by the glycerol double simultaneous adsorption on the Pt surface through both carbon atoms, C1, and C2, forming (1,3) dihydroxyacetone or glyceraldehyde, as the first oxidation step. One pathway leads to the formation of (1,3) dihydroxyacetone at *ca.* 0.6 V without forming CO_{ad} on the surface and, another possible pathway, forms glyceraldehyde which is a soluble intermediate that might produce CO_{ad}, that reacts via Langmuir-Hinshelwood mechanism in the presence of surface adsorbed oxygenated species to form CO_2 at 0.7 V [16,41]. A third pathway can occur if the initial bonding mode of glycerol to the Pt surface is simultaneous through the C1 and C3 carbons, leading to the direct oxidation to CO_2.

The potential oscillatory region observed in the GTS curves coincides with the potential region of the CV where CO linearly adsorbed, carbonyl, and carboxylic species are formed [41]. The potential stability region, in the GTS series (~ 0.60 V), indicates an accumulation of adsorbates on the electrode surface, once the kinetic of adsorbates production depends on the current density applied, leading to the oscillation appearance (see Fig. 6 A1 and A2) and the non-appearance (see Fig. 6 A3).

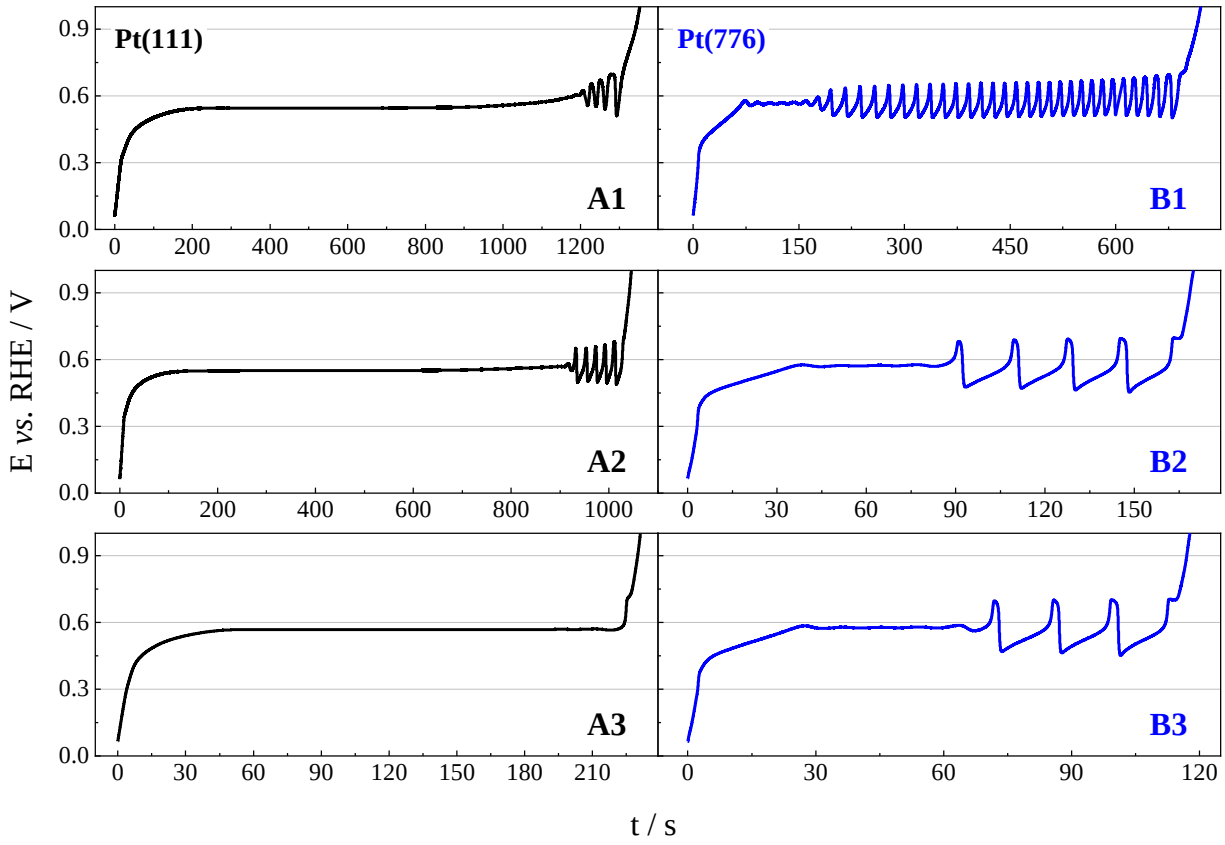

Fig. 6. Galvanostatic time series for glycerol electro-oxidation on Pt(111): (A1) 0.011, (A2) 0.022, (A3) 0.044 mA cm^{-2} and on Pt(776) at (B1) 0.025, (B2) 0.049 and (B3) 0.074 mA cm^{-2}. (0.5 M H_2SO_4 + 0.2 M Gly).

Fig. 6 also shows the GTS for GEOR on Pt(111) and Pt(776) surfaces. On a stepped surface, as is the case of Pt(776), the increase of potential observed at the beginning of GTS has two distinct behaviors. The potential increases abruptly until 0.45 V and then follow slowly up to *ca.* 0.60 V where oscillations rise. The oscillations obtained for this surface are similar to Pt(111), which emerges as the potential is close to 0.60 V, a period-1 oscillations are observed at *ca.* 0.57 V, with an amplitude of 0.25 V. The presence of (110) steps on Pt(776) surface, brings up other adsorption sites not present on Pt(111) surface. This structural modification influences the reaction mechanism forming different species and this needs to be considered to explain the emergence of oscillations observed on both surfaces. This change in the oscillation pattern also was observed on Pt(776) for methanol electro-oxidation reaction in acid electrolyte [20].

Fig. 7 shows the GTS for GEOR on Pt(554) under (A1) 0.011 (A2) 0.022 and (A3) 0.044 mA cm^{-2}. Initially, at 0.044 mA cm^{-2}, the potential increases faster up to 0.55 V, then an induction period before oscillation was slowly increased up to 0.75 V, and, finally, the oscillations started. For a current density of 0.011 mA cm^{-2}, the curve begins similar to the previous one, but the induction period is replaced by oscillations. Then, P1 appeared after the induction time and the oscillations decreased with each cycle. Finally, this type of oscillation was extinguished by the mixed oscillations. For the highest current density values, 0.22 and 0.044 mA cm^{-2}, only P1 oscillations were observed in the GTS for GEOR, normally observed for Pt polycrystalline case in the acid medium [12–14].

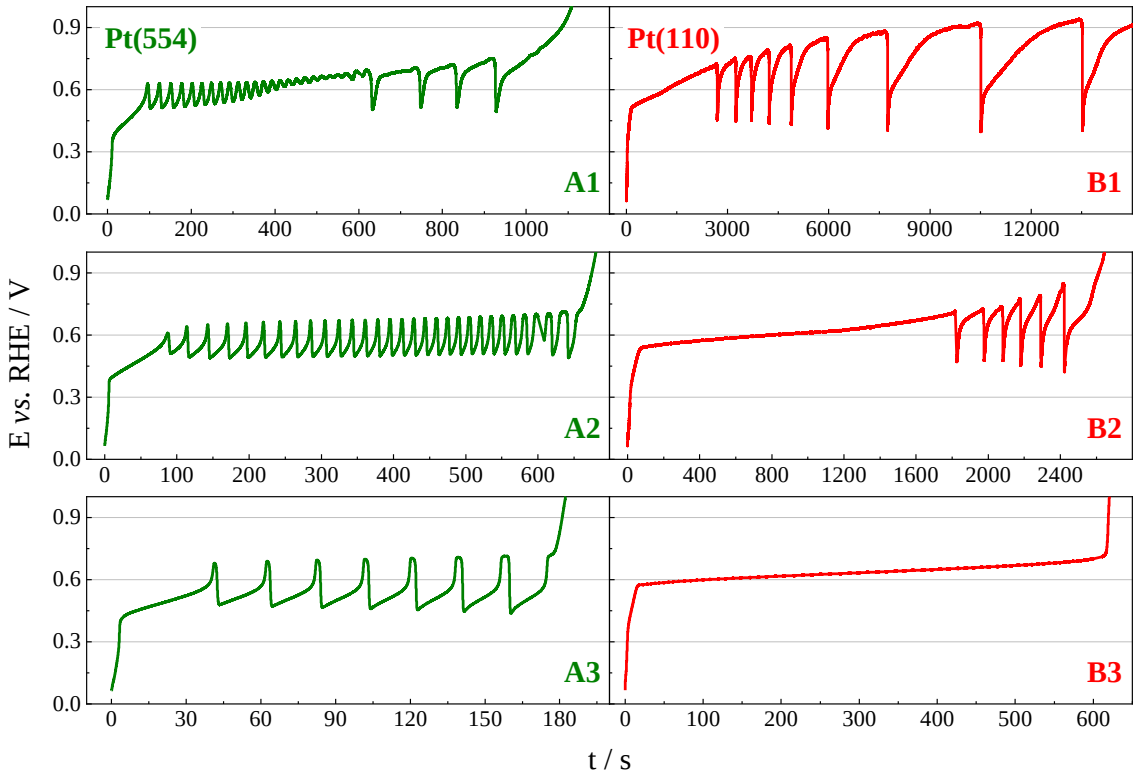

Fig. 7. Galvanostatic time series for glycerol electro-oxidation on Pt(554) at: (A1) 0.011 (A2) 0.022 and (A3) 0.044 mA cm^{-2} and on Pt(110) at: (B1) 0.0098 (B2) 0.0195 and (B3) 0.0587 mA cm^{-2} (0.5 M H_2SO_4 + 0.2 M Gly).

Fig. SI4 shows the GTS for glycerol electro-oxidation on Pt(332) surface under (A) 0.069 (B) 0.078 and (C) 0.083 mA cm^{-2}. For 0.069 mA cm^{-2}, the potential increases faster up to ~0.65 V, showing the first cycle, and an induction period to start at ~0.58V - 0.60V when the

oscillations emerged again more stable for ~220 seconds. Current densities of 0.078 and 0.083 mA cm^{-2}, the curve begins under oscillation cycles in the same amplitude of the last case, ~0.30 V, but the time series were shorter increasing the current density values. The oscillation pattern was P1 similar to previous related cases.

Fig. 7 also shows the GTS for GEOR on Pt(110) surface under (B1) 0.98, (B2) 19.5, (B3) 58.7 µA cm^{-2}. On this surface at the beginning of the GTS, the potential increases rapidly to around 0.55 V, following a slower increase up to 0.7 V, where oscillations emerged. Herein the oscillations are slower with higher amplitude (*ca.* 0.45 V) as compared to other surfaces. Also, Pt(110) showed oscillations and series with the longest time of duration among all surfaces studied, except B3. For two applied currents (B1 and B2) the frequency of oscillations varied over time and gradually increased the amplitude. However, the frequency diminished with the time at 0.0098 µA cm^{-2}, and the opposite behavior was noted in the case of 0.0195 µA cm^{-2}.

3.4 Remarks on the oscillatory electro-oxidation of glycerol

Two peak currents are observed for the GEOR on Pt(111), Pt(776), Pt(554), and Pt(332) at 0.57 (peak I) and 0.70 V (peak II) in the positive sweep of the CV, the exception is for Pt(110) that has only one less pronounced peak at ca. 0.8 V [9]. Peak I is formed due to glycerol molecule oxidation and, peak II is assigned to poison oxidation, namely, ketone and/or aldehydes species and adsorbed CO [9,13,41]. During the GEOR on Pt(111) surface, the initial adsorption bonding mode of glycerol on the Pt surface determines the formation of the first oxidation product. If the surface bonding occurs simultaneously through the C1 and C2 carbons, glyceraldehyde or (1,3)dihydroxyacetone is formed. In turn, further oxidation of glyceraldehyde and (1,3)dihydroxyacetone oxidations follow two different pathways, both leading to CO_2 production, yet with a slow kinetic reaction. In the case of ketone, its oxidation

produces hydroxypyruvic acid that is slowly oxidized to CO_2. In contrast, a small amount of glyceraldehyde might be responsible for forming species that come from breaking of the C–C bond and, consequently, forming strongly adsorbed species such as CO that is partially converted to CO_2 [41].

An interesting point highlighted by Melle et al. [13] about peaks I and II, refers to the fact that it was observed only the peak II for Pt polycrystalline, using a rotating disk electrode (RDE) for GEOR, under stationary conditions. The effect of mass transport in the GEOR affects the reaction [13], where the RDE removes soluble intermediates (glyceraldehyde) unable to re-adsorb again, thus, hindering the reaction pathway resulting from the C–C break and, consequently, the formation of CO_{ads}. Concerning oscillations, the authors observed that the rotation of the electrode leads to the removal of the glyceraldehyde and the oscillations extinction.

Therefore, the potential oscillatory behavior resulting during the GEOR is presumably associated with the formation of adsorbed CO on the surface. In our experiments, differently from what was observed from a rotating procedure, the intermediate formed remains near the surface, consequently, a long induction period is seen before starting the short oscillations, this fact might be associated with slow poisoning on the surface. Therefore, short potential oscillations observed after the induction period, reveal that the intermediates formed are rapidly removed from the surface. This explains the high current densities observed in the CV for a surface having “infinitely wide” (111) terraces than stepped surfaces, once more carbonyl (C=O) species are formed on Pt(111) as was seen in FTIR studies [9].

In this sense, we believe that the Pt(111) is not very selective to form adsorbed CO. In other words, Pt(111) oxidizes glycerol, at low potential, mainly to form active species, that is, species that do not inhibit the glycerol oxidation reaction, such as 1,3 dihydroxyacetone and hydroxypyruvic acid. Another important point that agrees with this analysis is the high

proportion between the FTIR band intensities of the C=O and CO_2 [9] when monitoring the progress of the glycerol reaction on Pt(111) by FTIR. The low reaction kinetic for CO_2 formation comes from the previous formation of ketone, causing high values of C=O/CO_2 [9]. On this surface, the inactive intermediates are responsible for the poisoning with low reaction kinetic, probably, Pt(111) forms a low amount of glyceraldehyde, so the glycerol can be oxidized without poisoning species and, as consequence, emerging the peak I.

In contrast to that observed for Pt(111) electrode, the predominance of oscillatory kinetics observed in stepped surfaces are assigned to increase of inactive species, resulting from the incomplete oxidation of glycerol produced by breaking C–C bonds, then the introduction of (110) monoatomic steps promote these pathways. For Pt(554), the FTIR band intensities of the C=O/CO_2 ratio are less than that observed for surface (111), due to the increased species with C2 and C1 fragments, which had a more efficient CO_2 yield when compared to (111) surface. Such species inhibit the surface and compete for catalytic sites in the same potential region, providing oscillations observed in the GTS.

Finally, the differences observed on the Pt(110) surface can be rationalized as follows. The increase in the step density contributes to oscillation stability, probably, due to the greater selectivity for the glyceraldehyde formation, species responsible for forming adsorbed CO on the surface. Pt(110) also showed characteristics different from other surfaces, with a unique oscillatory pattern. This fact is probably linked to a differentiated selectivity in the reaction mechanism on that surface. A reasonable explanation might be done based on the opposite behavior to Pt(111), herein the onset potential is shifted to more positive potentials and, thus, the surface is covered by species strongly adsorbed. This surface seems to favor easier the C–C bond at low potential, FTIR results confirmed this assumption [9]. Another important point is the oscillatory pattern distinction on the Pt(110) compared to the other studied surfaces, which the results show us a profile utterly different; this surface needed to reach higher potential

values to carry out the surface cleaning, and its contamination reached lower potentials, showing that significant contamination by species strongly adsorbed on this surface. These facts are probably the reason for the difference between the oscillatory patterns on different surfaces.

The influence of Pt surface orientation on the oscillatory instabilities was observed for methanol electro-oxidation reaction [20]. The authors observed that the reaction rates of the electro-oxidation of methanol increase with the density of (110) sites and, consequently, the oscillations potentials are quite different among the surfaces. Although we are mentioning the behavior of a simple molecule like methanol, a comparison with glycerol may be inappropriate, since the number of intermediates formed is numerous and with different characteristics, but in general, it is observed that the stepped surfaces have a greater ability to produce adsorbed CO than the basal planes, Pt(*hkl*), and in a way, this trend remains the same here, which the (110) monoatomic steps contributed to the peculiar emergence of potential oscillations on these surfaces.

4. Conclusions

In the present study, we have shown for the first time the electrochemical behavior of Pt(*hkl*) and stepped surfaces towards the glycerol electro-oxidation reaction in sulfuric acid aqueous solution. Cyclic voltammetry has demonstrated the strong influence of bi(sulfate) anions over GEOR, the electrolyte concentration affects negatively the performance of all surfaces studied, in this case, the anion adsorption plays an outstanding effect over glycerol adsorption and its posterior oxidation. Chronoamperometric experiments demonstrated that the Pt(111) surface is very active at 0.60 V, but when the potentials make more positive, the surfaces are greatly poisoned by intermediates strongly adsorbed. The stepped surfaces follow the same trend, while Pt(110) presents an opposite effect, where the current densities increase

as the potential increases, confirming that this surface has more ability in breaking the C–C bond.

Potential oscillations were observed for the GEOR mainly on Pt(776), Pt(554) and Pt(110) surfaces. For galvanostatic conditions, oscillations emerge for Pt(111) after a long induction period, where the surface was poisoned by species strongly adsorbed and, thus, causing the beginning of the oscillation. For Pt(776) and Pt(554) surfaces potential oscillations emerge, indicating a route formed by intermediates that poison the surface as demonstrated in the CVs.

Acknowledgments

The authors acknowledge FAPESP (Grants Nº. #2013/16930-7 and #2019/22183-6), FAPEAL (process 60030-001076/2016), CAPES - Brasil (CAPES, Grant Nº. 0001, and for the scholarship, GBM, #88887.341974/2019-00). HV (Grant Nº. 306060/2017-5) and GTF (Grant N° 313455/2021-0) acknowledge CNPq for financial support. We gratefully acknowledge the support of the RCGI – Research Centre for Gas Innovation, hosted by the University of São Paulo (USP) and sponsored by FAPESP (2014/50279-4 and 2020/15230-5) and Shell Brazil, and the strategic importance of the support given by ANP (Brazil's National Oil, Natural Gas, and Biofuels Agency) through the R&D levy regulation.

References

[1] O.A. Petrii, The Progress in Understanding the Mechanisms of Methanol and Formic Acid Electrooxidation on Platinum Group Metals (a Review), Russ. J. Electrochem. 55 (2019) 1–33. https://doi.org/10.1134/S1023193519010129.

[2] C.A. Angelucci, J. Souza-Garcia, P.S. Fernández, P.V.B. Santiago, R.M.L.M. Sandrini, Glycerol Electrooxidation on Noble Metal Electrode Surfaces, in: Encycl. Interfacial Chem., Elsevier, 2018: pp. 643–650. https://doi.org/10.1016/B978-0-12-409547-2.13330-X.

[3] P.A. Alaba, C.S. Lee, F. Abnisa, M.K. Aroua, P. Cognet, Y. Pérès, W.M.A. Wan Daud, A review of recent progress on electrocatalysts toward efficient glycerol electrooxidation, Rev. Chem. Eng. (2020). https://doi.org/10.1515/revce-2019-0013.

[4] F. Yang, J.Y. Ye, Q. Yuan, X. Yang, Z. Xie, F. Zhao, Z. Zhou, L. Gu, X. Wang, Ultrasmall Pd-Cu-Pt Trimetallic Twin Icosahedrons Boost the Electrocatalytic Performance of Glycerol Oxidation at the Operating Temperature of Fuel Cells, Adv. Funct. Mater. 30 (2020) 1–9. https://doi.org/10.1002/adfm.201908235.

[5] M.R. Rizk, M.G. Abd El-Moghny, G.A. El-Nagar, A.A. Mazhar, M.S. El-Deab, Tailor-Designed Porous Catalysts: Nickel-Doped Cu/Cu2O Foams for Efficient Glycerol Electro-Oxidation, ChemElectroChem. 7 (2020) 951–958. https://doi.org/10.1002/celc.201902166.

[6] S. Bagheri, N.M. Julkapli, W.A.Y. Dabdawb, N. Mansouri, Biodiesel -Derived Raw Glycerol to Value-Added Products: Catalytic Conversion Approach, in: Handb. Compos. from Renew. Mater., John Wiley & Sons, Inc., Hoboken, NJ, USA, 2017: pp. 309–365. https://doi.org/10.1002/9781119441632.ch52.

[7] H.A. Miller, A. Lavacchi, F. Vizza, Storage of renewable energy in fuels and chemicals through electrochemical reforming of bioalcohols, Curr. Opin. Electrochem. 21 (2020)

140–145. https://doi.org/10.1016/j.coelec.2020.02.001.

[8] Y. Holade, N. Tuleushova, S. Tingry, K. Servat, T.W. Napporn, H. Guesmi, D. Cornu, K.B. Kokoh, Recent advances in the electrooxidation of biomass-based organic molecules for energy, chemicals and hydrogen production, Catal. Sci. Technol. 10 (2020) 3071–3112. https://doi.org/10.1039/C9CY02446H.

[9] V. Del Colle, L.M.S. Nunes, C.A. Angelucci, J.M. Feliu, G. Tremiliosi-Filho, The influence of stepped Pt[n(111)×(110)] electrodes towards glycerol electrooxidation: Electrochemical and FTIR studies, Electrochim. Acta. 346 (2020) 136187. https://doi.org/10.1016/j.electacta.2020.136187.

[10] L. Carrette, K.A. Friedrich, U. Stimming, Fuel Cells - Fundamentals and Applications, Fuel Cells. 1 (2001) 5–39. https://doi.org/10.1002/1615-6854(200105)1:1<5::AID-FUCE5>3.0.CO;2-G.

[11] E.G. Machado, H. Varela, Kinetic Instabilities in Electrocatalysis, in: Encycl. Interfacial Chem., Elsevier, 2018: pp. 701–718. https://doi.org/10.1016/B978-0-12-409547-2.13369-4.

[12] C.P. Oliveira, N. V. Lussari, E. Sitta, H. Varela, Oscillatory electro-oxidation of glycerol on platinum, Electrochim. Acta. 85 (2012) 674–679. https://doi.org/10.1016/j.electacta.2012.08.087.

[13] G.B. Melle, E.G. Machado, L.H. Mascaro, E. Sitta, Eff ect of mass transport on the glycerol electro-oxidation, Electrochim. Acta. 296 (2019) 972–979. https://doi.org/https://doi.org/10.1016/j.electacta.2018.11.085.

[14] G.B. Melle, T. Altair, R.L. Romano, H. Varela, Electrocatalytic Efficiency of the Oxidation of Ethylene Glycol, Glycerol, and Glucose under Oscillatory Regime, Energy & Fuels. 35 (2021) 6202–6209. https://doi.org/10.1021/acs.energyfuels.1c00203.

[15] G. Melle, M. de Souza, P.V.B. Santiago, P.G. Corradini, L.H. Mascaro, P.S. Fernández,

E. Sitta, Glycerol Electro-Oxidation at Pt in Alkaline Media – Influence of Mass Transport and Cations., Electrochim. Acta. (2021) 139318. https://doi.org/10.1016/j.electacta.2021.139318.

[16] Y. Kwon, K.J.P. Schouten, M.T.M. Koper, Mechanism of the Catalytic Oxidation of Glycerol on Polycrystalline Gold and Platinum Electrodes, ChemCatChem. 3 (2011) 1176–1185. https://doi.org/10.1002/cctc.201100023.

[17] J. Clavilier, D. Armand, S.G. Sun, M. Petit, Electrochemical adsorption behaviour of platinum stepped surfaces in sulphuric acid solutions, J. Electroanal. Chem. Interfacial Electrochem. 205 (1986) 267–277. https://doi.org/10.1016/0022-0728(86)90237-8.

[18] C. Korzeniewski, V. Climent, J. Feliu, Electrochemistry at Platinum Single Crystal Electrodes, in: 2011: pp. 75–170. https://doi.org/10.1201/b11480-3.

[19] E. Herrero, J.M. Orts, A. Aldaz, J.M. Feliu, Scanning tunneling microscopy and electrochemical study of the surface structure of Pt(10,10,9) and Pt(11,10,10) electrodes prepared under different cooling conditions, Surf. Sci. 440 (1999) 259–270. https://doi.org/10.1016/S0039-6028(99)00813-4.

[20] V. Del Colle, P.B. Perroni, J.M. Feliu, G. Tremiliosi-Filho, H. Varela, The Role of Surface Sites on the Oscillatory Oxidation of Methanol on Stepped Pt[n(111) × (110)] Electrodes, J. Phys. Chem. C. 124 (2020) 10993–11004. https://doi.org/10.1021/acs.jpcc.0c01897.

[21] E. Herrero, J. Mostany, J.M. Feliu, J. Lipkowski, Thermodynamic studies of anion adsorption at the Pt(111) electrode surface in sulfuric acid solutions, J. Electroanal. Chem. 534 (2002) 79–89. https://doi.org/10.1016/S0022-0728(02)01101-4.

[22] Z. Su, V. Climent, J. Leitch, V. Zamlynny, J.M. Feliu, J. Lipkowski, Quantitative SNIFTIRS studies of (bi)sulfate adsorption at the Pt(111) electrode surface, Phys. Chem. Chem. Phys. 12 (2010) 15231. https://doi.org/10.1039/c0cp00860e.

[23] N.M. Marković, N.S. Marinković, R.R. Adžić, Electrosorption of hydrogen and sulfuric acid anions on single crystal platinum stepped surfaces, J. Electroanal. Chem. Interfacial Electrochem. 314 (1991) 289–306. https://doi.org/10.1016/0022-0728(91)85443-S.

[24] F.C. Nart, T. Iwasita, M. Weber, Vibrational spectroscopy of adsorbed sulfate on Pt(111), Electrochim. Acta. 39 (1994) 961–968. https://doi.org/10.1016/0013-4686(94)85113-1.

[25] T. Iwasita, F.C. Nart, A. Rodes, E. Pastor, M. Weber, Vibrational spectroscopy at the electrochemical interface, Electrochim. Acta. 40 (1995) 53–59. https://doi.org/10.1016/0013-4686(94)00239-W.

[26] N.M. Marković, N.S. Marinković, R.R. Adžić, Electrosorption of hydrogen and sulphuric acid anions on single-crystal platinum stepped surfaces, J. Electroanal. Chem. Interfacial Electrochem. 241 (1988) 309–328. https://doi.org/10.1016/0022-0728(88)85134-9.

[27] T. Haisch, F. Kubannek, L. Nikitina, I. Nikitin, S. Pott, T. Clees, U. Krewer, The origin of the hysteresis in cyclic voltammetric response of alkaline methanol electrooxidation, Phys. Chem. Chem. Phys. 22 (2020) 16648–16654. https://doi.org/10.1039/D0CP00976H.

[28] M.T.M. Koper, S.C.S. Lai, E. Herrero, Mechanisms of the Oxidation of Carbon Monoxide and Small Organic Molecules at Metal Electrodes, in: Fuel Cell Catal., John Wiley & Sons, Inc., Hoboken, NJ, USA, 2008: pp. 159–207. https://doi.org/10.1002/9780470463772.ch6.

[29] R.M. Arán-Ais, E. Herrero, J.M. Feliu, The breaking of the CC bond in ethylene glycol oxidation at the Pt(111) electrode and its vicinal surfaces, Electrochem. Commun. 45 (2014) 40–43. https://doi.org/10.1016/j.elecom.2014.05.008.

[30] V.S. Bagotzky, Y.B. Vassilyev, J. Weber, J.N. Pirtskhalava, Adsorption of anions on

smooth platinum electrodes, J. Electroanal. Chem. Interfacial Electrochem. 27 (1970) 31–46. https://doi.org/10.1016/S0022-0728(70)80200-5.

[31] V. Del Colle, A. Berná, G. Tremiliosi-Filho, E. Herrero, J.M. Feliu, Ethanol electrooxidation onto stepped surfaces modified by Ru deposition: electrochemical and spectroscopic studies, Phys. Chem. Chem. Phys. 10 (2008) 3766. https://doi.org/10.1039/b802683a.

[32] F. Colmati, G. Tremiliosi-Filho, E.R. Gonzalez, A. Berná, E. Herrero, J.M. Feliu, The role of the steps in the cleavage of the C–C bond during ethanol oxidation on platinum electrodes, Phys. Chem. Chem. Phys. 11 (2009) 9114. https://doi.org/10.1039/b907250k.

[33] A.C. Garcia, J. Caliman, E.B. Ferreira, G. Tremiliosi-filho, J.J. Linares, Promotional Effect of Ag on the Catalytic Activity of Au for Glycerol Electrooxidation in Alkaline Medium, (2015) 1036–1041. https://doi.org/10.1002/celc.201500022.

[34] P.S. Fernández, P. Tereshchuk, C.A. Angelucci, J.F. Gomes, A.C. Garcia, C.A. Martins, G.A. Camara, M.E. Martins, J.L.F.F. Da Silva, G. Tremiliosi-Filho, How do random superficial defects influence the electro-oxidation of glycerol on Pt(111) surfaces?, Phys. Chem. Chem. Phys. 18 (2016) 25582–25591. https://doi.org/10.1039/c6cp04768h.

[35] G.L. Caneppele, C.A. Martins, Revisiting glycerol electrooxidation by applying derivative voltammetry: From well-ordered bulk Pt to bimetallic nanoparticles, J. Electroanal. Chem. 865 (2020) 114139. https://doi.org/10.1016/j.jelechem.2020.114139.

[36] J. Mostany, E. Herrero, J.M. Feliu, J. Lipkowski, Thermodynamic Studies of Anion Adsorption at Stepped Platinum(h kl) Electrode Surfaces in Sulfuric Acid Solutions, J. Phys. Chem. B. 106 (2002) 12787–12796. https://doi.org/10.1021/jp026561p.

[37] I.A. Fiori, G.B. Melle, E. Sitta, Halide adsorption effect on methanol electro-oxidation reaction studied by dynamic instabilities, J. Electroanal. Chem. 856 (2020) 113657.

https://doi.org/10.1016/j.jelechem.2019.113657.

[38] R. Nagao, I.R. Epstein, E.R. Gonzalez, H. Varela, Temperature (Over)Compensation in an Oscillatory Surface Reaction, J. Phys. Chem. A. 112 (2008) 4617–4624. https://doi.org/10.1021/jp801361j.

[39] G.B. Melle, F.W. Hartl, H. Varela, E. Sitta, The effect of solution pH on the oscillatory electro-oxidation of methanol, J. Electroanal. Chem. 826 (2018) 164–169. https://doi.org/10.1016/j.jelechem.2018.08.033.

[40] M.G. de Oliveira, G.B. Melle, R.L. Romano, H. Varela, The Impact of Water Concentration on the Electro-Oxidation of Formic Acid on Platinum, J. Electrochem. Soc. 169 (2022) 026514. https://doi.org/10.1149/1945-7111/ac5060.

[41] A.C. Garcia, M.J. Kolb, C. van Nierop y Sanchez, J. Vos, Y.Y. Birdja, Y. Kwon, G. Tremiliosi-Filho, M.T.M. Koper, Strong Impact of Platinum Surface Structure on Primary and Secondary Alcohol Oxidation during Electro-Oxidation of Glycerol, ACS Catal. 6 (2016) 4491–4500. https://doi.org/10.1021/acscatal.6b00709.